A new type of microfluidic-metamaterial fusion terahertz sensor

JIANJUN LIU[1], TIEJUN LI[2], LANLAN FAN[1], FANG DING[1], SENQUAN YANG[1]
[1]*School of Intelligent Engineering, Shaoguan University, Shaoguan Guangdong 363000, China*
[2]*College of Information Engineering, Jimei University, Fujian Province, Xiamen 361021, China*

A new type of terahertz sensor with microfluidic and metamaterial fusion is designed in this paper. Taking ethanol aqueous solution as the research object, the terahertz spectra of ethanol aqueous solution with different mole fraction were analyzed and studied. With the increase of mole fraction, the terahertz resonance absorption frequency of ethanol solution decreases gradually, while the resonance summit appears blue shift to varying degrees. The quantitative detection of the mole fraction can be realized through the corresponding relationship between the blue shift of the resonance absorption peak and the mole fraction. The research results of this paper are helpful to promote the application of terahertz time domain spectroscopy in rapid, micro and real-time material identification and biosensor.

(Received September 22, 2022; accepted December 6, 2022)

Keywords: terahertz, sensor, microfluidic, Metamaterial

1. Introduction

Terahertz biosensor is a research hotspot in terahertz functional devices. Through the biosensor, not only the samples of different components can be detected conveniently, but also the chemical reactions between biomolecules and drugs can be monitored. Therefore, the development of terahertz biosensors with high sensitivity has important research value and significance. At present, terahertz biosensors are mostly made of metamaterials. Metamaterials are artificially designed structures in the sub-wavelength range [1-3]. Metamaterials have extraordinary physical properties, which can realize the artificial control of electromagnetic waves to a certain extent. The biosensor technology in terahertz band is not yet mature, and its main difficulty is to overcome the strong absorption of terahertz wave by water. The early work is to use metamaterials as sensors to realize the sensing detection of biological proteins [4] and antibiotics [5-6] which are attached to the surface of metamaterials after drying. However, the practicability of the above method is limited because the solution environment of the dried sample is very different from that of the actual organism. In order to maintain the solution environment of the organism, reducing the thickness of the solution as much as possible is an effective way to reduce the terahertz wave absorption of water. Researchers put metamaterials in solution cavities to explore their applications in drug reaction monitoring [7] and mixture detection [8], but quantitative detection is still very difficult. The microfluidic chip technology developed in recent years provides a new way for the fabrication of terahertz biosensors [9-15]. Microfluidic chip technology can accurately control the microfluidic channel at the micron level, which is an ideal choice for the fabrication of terahertz biosensors. In recent years, microfluidic chips have been used in the sensing detection of isopropanol-water and acetonitrile-water mixtures in terahertz band [16] and the detection of specific virus samples[17]. However, using the microchannel as the sensor, the measurement results are not intuitive enough, which increases the difficulty for the analysis of the results. Therefore, by combining the metamaterial with specific resonance response with the microfluidic chip, the change of liquid characteristics in the microchannel can be easily observed by observing the movement of the metamaterial formant in the frequency spectrum. In 2016, several research groups at home and abroad tried to integrate metamaterials into microfluidic chips for the detection of different organic solutions [18] and glucose solutions [19-20]. Recently, part of the work has also shown its development potential in liver cancer diagnosis [21] and biosensor [22]. A new type of microfluidic-metamaterial terahertz sensor is designed in this paper. By detecting the absorption spectra of ethanol solutions with different mole fractions, the quantitative relationship between the frequency and absorptivity of the four formants of the sensor and the mole fraction of ethanol was obtained and applied to the determination of the mole fraction of ethanol aqueous solution.

2. Sensor structure design

A new type of microfluidic-metamaterial integrated terahertz sensor is designed in this paper. The terahertz sensor has a three-layer structure, as shown in Fig. 1 (a).

The top structure consists of a quartz substrate and a metamaterial structure plated on its lower surface (the material is gold), and the bottom structure is a silicon substrate. The metamaterial of the top structure is a two-dimensional periodic array structure in the x-y plane. The unit structure is shown in Fig. 1 (b), and each element contains four identical L-shaped metal structures. The length of the three arms of the L-shaped metal structure is 55μm, the interval between the two L-shaped arms is 2μm, the linewidth of all metal structures is 2μm, the period of the unit in the x and y directions is 112 μm, the thickness of the metal layer is 0.2 μm, the thickness of the substrate is 200 μm, and the height of the microfluidic channel is 30 μm.

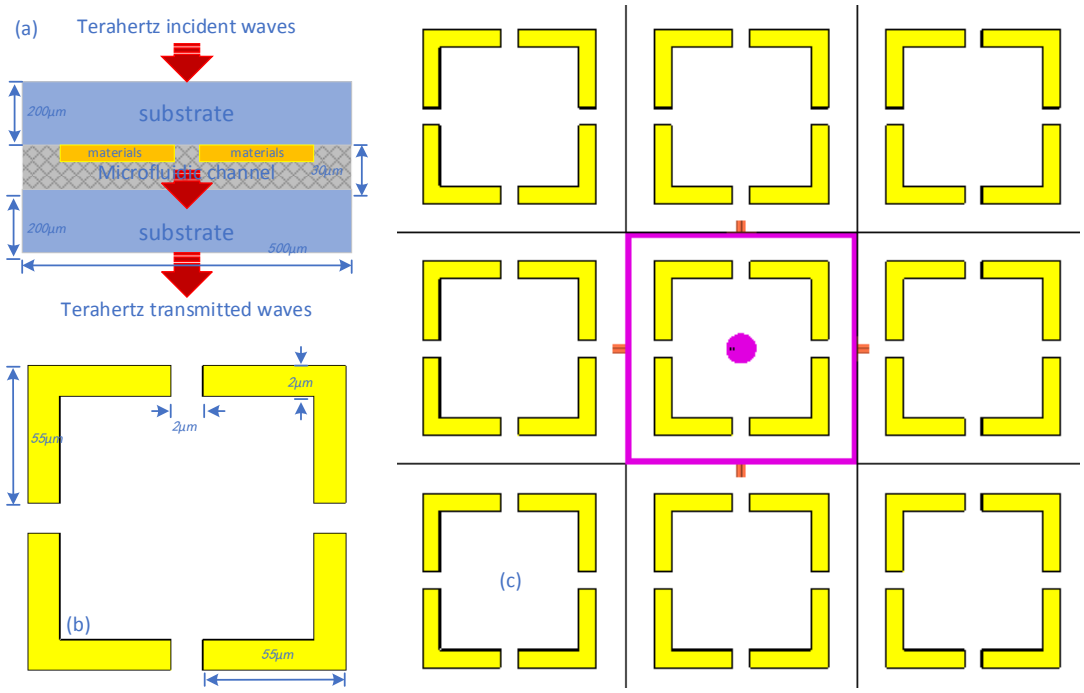

Fig. 1. Schematic diagram of the structure of the sensor designed:(a) sensor side view; (b) sensor cover structure metamaterial element; (c) metamaterial element periodic array

3. Simulation calculation and modeling method

In this paper, CST (Computer Simulation Technology) microwave laboratory [23] is used to simulate the sensor. The polarized terahertz wave along the y-axis is incident from the top layer along the z-axis to the top layer of the sensor. In order to eliminate the influence of terahertz reflection echo in the top substrate, a perfectly matched layer is set up on the incident (exit) surface, and the absorption spectrum is calculated. In the simulation calculation, the conductivity of gold is set to 4.52 × 107S/m [24], and the dielectric constant of silicon is set to 3.82 [25]. The material in microfluidic is set to air or medium (such as ethanol aqueous solution). In this paper, Debye model is used to describe the complex permittivity $\varepsilon_m(\omega)$ of ethanol and water [26-27]:

$$\varepsilon_m(\omega) = \varepsilon_\infty + \sum_i^n \frac{\varepsilon_i - \varepsilon_{i+1}}{1 + j\omega\tau_i} \tag{1}$$

In the formula, ω represents the angular frequency and i represents the order (take the integer), n as the total order, ε_i as the dielectric constant, ε_∞ as the high frequency limit and τ_i as the relaxation time. The Debye model parameters of ethanol and water are shown in Table 1.

Table 1. Debye model of ethanol and water

Liquid	ε_1	τ_1(ps)	ε_2	τ_2(ps)	ε_3	τ_3(ps)	ε_∞
Ethanol	23.45	153	5.14	3.12	2.89	0.34	1.76
Water	73.86	8.42	5.39	0.26			

By changing the mixing ratio of ethanol and water [28], the dielectric constant $\varepsilon_m(\omega)$ of ethanol aqueous

solution with different mole fraction can be obtained.

$$\varepsilon_m(\omega)=\zeta\varepsilon_e(\omega)+(1-\zeta)\varepsilon_w(\omega) \tag{2}$$

In the formula, ζ represents the concentration of ethanol in the solution, $\varepsilon_e(\omega)$ and $\varepsilon_w(\omega)$ represent the dielectric constant of ethanol and water, respectively. The dispersion curves of the real and imaginary parts of the permittivity of ethanol aqueous solution can be obtained from the above formula, as shown in Fig. 2 (a). At the same time, the relationship between refractive index $n(\omega)$, extinction coefficient $\kappa(\omega)$, absorption coefficient $\alpha(\omega)$ and dielectric constant [29]:

$$\begin{cases} n^2(\omega)-\kappa^2(\omega)=\mathrm{Re}\left[\varepsilon_m(\omega)\right] \\ 2n(\omega)\kappa(\omega)=\mathrm{Im}\left[\varepsilon_m(\omega)\right] \\ \alpha(\omega)=2\omega\kappa(\omega)/c \end{cases} \tag{3}$$

In the formula, $\varepsilon_m(\omega)$ is the dielectric constant of the mixed solution and c is the speed of light in vacuum. The dispersion curves of refractive index and absorption coefficient of aqueous ethanol solutions with different concentrations can be extracted from the above formula, as shown in Fig. 2 (b), respectively. Because the refractive index and absorption coefficient of water are larger than those of ethanol, the refractive index and absorption coefficient of ethanol aqueous solution decrease with the increase of ethanol mole fraction.

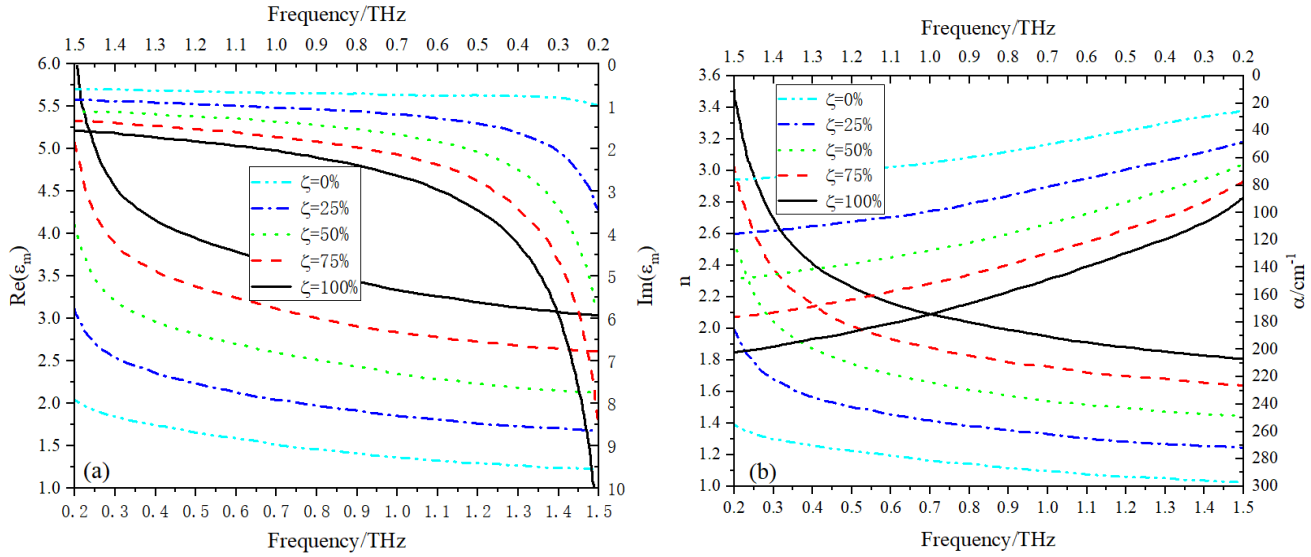

Fig. 2. Dispersion curves of aqueous ethanol solutions with different concentrations the real and imaginary parts of (a) dielectric constant; (b) refractive index and absorption coefficient

The multi-layer structure design of the sensor makes a part of the incident terahertz wave reflect many times between the metal microstructure layer and the metal reflector, and this part of the terahertz wave is bound in the microflow channel to form F-P resonance, so as to realize the absorption of terahertz wave. The intensity of resonant absorption depends on the degree of matching between the equivalent impedance of the sensor and the impedance of the free space. by adjusting the height of the microflow channel, the equivalent impedance of the sensor can be changed to make it match well with the impedance of the free space. so as to enhance the absorption of terahertz waves. For this reason, under the condition that other parameters are constant, the effect of different height (h =0 ~50μm) microflow channel on the absorption peak absorptivity of the sensor is studied. The simulation results are shown in Fig. 3.

As can be seen from the figure, the absorptivity of the resonant peak of the sensor varies with the height of the microfluidic channel. When the height of the microfluidic channel is 30μm, the equivalent impedance of the sensor is closest to the impedance of free space, and the impedance matching effect is the best. The absorptivity of low-frequency and high-frequency resonant peaks of the sensor reaches the maximum.

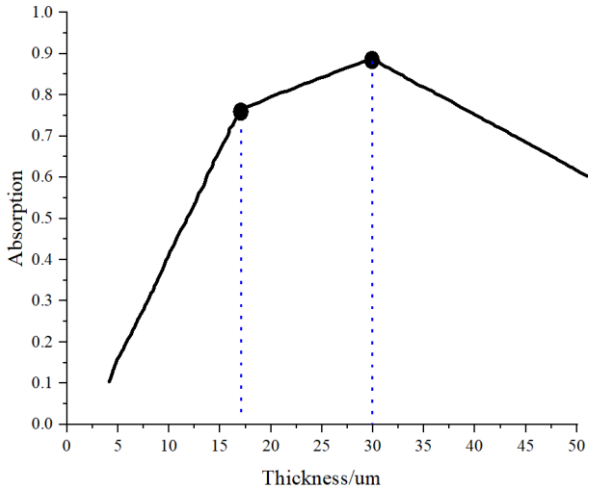

Fig. 3. Effect of microflow channel height on absorptivity

4. Results and discussion

When the terahertz wave is incident from the cover and there is air in the microfluidic channel, the transmission spectrum of the sensor is shown in Fig. 4.

At this time, the transmission spectrum has four resonance absorption peaks in the effective detection band, which are marked as *peak 1*, *peak 2*, *peak 3* and *peak 4* from low frequency to high frequency, respectively.

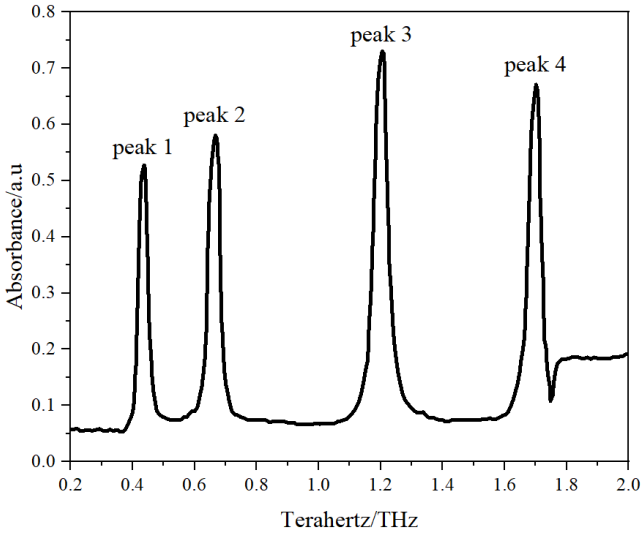

Fig. 4. Terahertz absorption response of sensor

In order to further analyze the detection sensitivity of the microfluidic-metamaterial sensor, this paper simulates the absorption spectrum of the sensor when the microfluidic channel is filled with non-absorbing media with different refractive index. As shown in Fig. 5 (a), when the refractive index of the medium in the microfluidic channel is gradually changed from 1 to 2, the four resonance absorption peaks of the sensor can be observed to red shift at the same time. The sensitivity of the four formants of the sensor is calculated by using the sensitivity formula.

$$S=\Delta f / \Delta n \tag{4}$$

In the formula, Δf is the resonant peak frequency shift and Δn is the refractive index change. From the sensitivity results shown in Fig. 5 (b), it can be seen that the sensitivity of the highest frequency formant *peak 4* of the designed sensor is 192GHz/RIU (RIU is Refractive Index Unit). Therefore, when it is applied to the detection of ethanol aqueous solution with great difference in dielectric constant, the obvious resonance peak frequency shift can be observed.

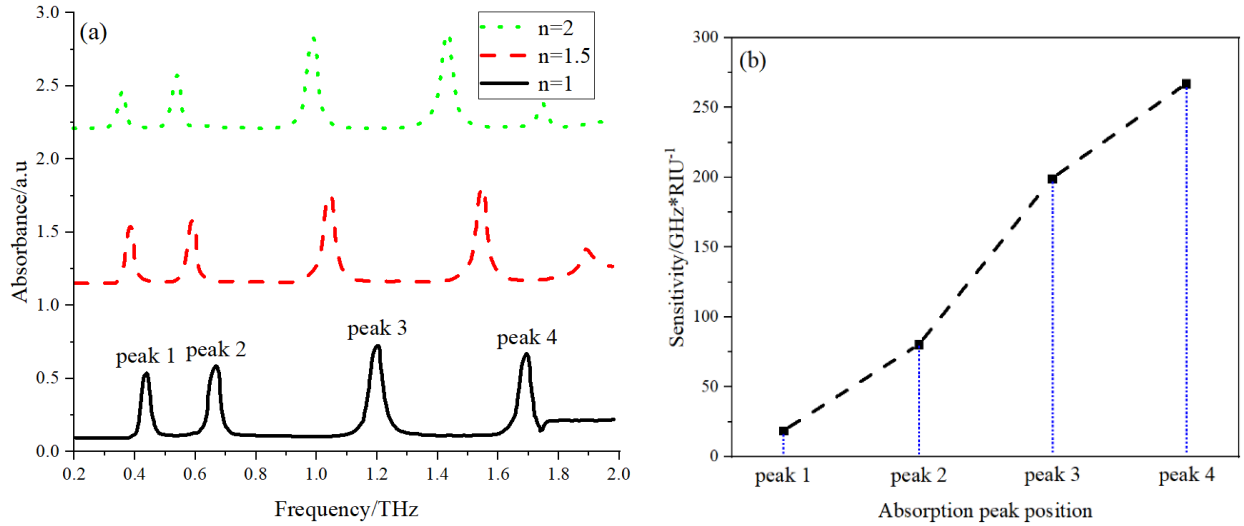

Fig. 5. Absorption spectrum and sensitivity of the sensor.(a) Absorption Spectrum with different Refractive Index of Media in Microfluidic Channel of Sensor; (b) Sensitivity of each absorption peak of the sensor

The complex permittivity of ethanol aqueous solution is calculated according to $\varepsilon_m(\omega)=\zeta\varepsilon_e(\omega)+(1-\zeta)\varepsilon_w(\omega)$, which is set as the medium parameter in the microfluidic channel of the sensor, and the corresponding absorption spectrum is calculated. The result is shown in Fig. 6 (a). Fig. 6 (b) shows the relationship between the absorptivity of the sensor and the concentration of ethanol.

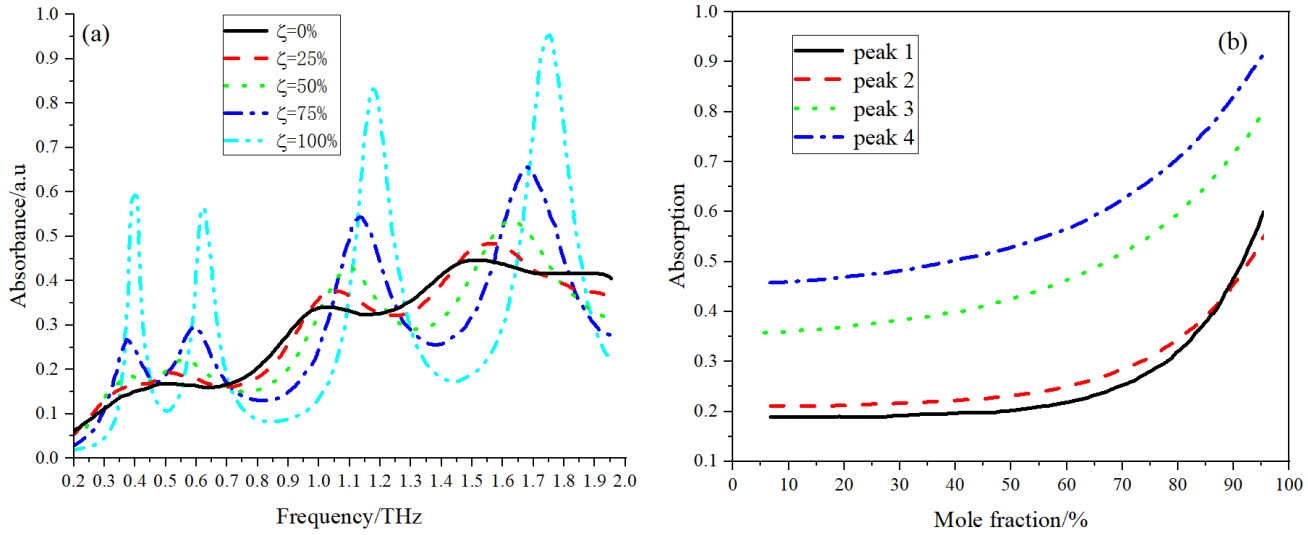

Fig. 6. (a) Reflection spectrum of the sensor for aqueous ethanol solution with different mole fraction of ethanol; (b) the relationship between the formant reflectivity of the sensor and the mole fraction of ethanol

The dispersion curve of the refractive index and absorption coefficient of ethanol aqueous solution [see Fig. 2 (b)] shows that when the ethanol concentration increases gradually, the refractive index of ethanol aqueous solution decreases and the absorption coefficient increases, so the peak position of the four formant peaks in the absorption spectrum gradually blue shifts, the Q value of the formant peak increases, and the absorptivity decreases gradually. It should be pointed out that due to the close distance between peak 1 and 2 at low frequency, when the mole fraction of ethanol is low, the Q value of the formant decreases, that is, the linewidth increases, which will lead to the difficulty of distinguishing the two peaks.

5. Conclusion

A new type of microfluidic metamaterial integrated multi-band terahertz sensor is designed in this paper. The sensor consists of a metal plate at the bottom, a metamaterial in the cover layer, and a microfluidic channel between them. The absorption spectrum of the sensor in detecting ethanol aqueous solution with different mole fraction was simulated. The results show that with the increase of the mole fraction of ethanol, the amplitudes of the four formants in the absorption spectrum gradually decrease, while the peak positions gradually blue shift. The relationship between the mole fraction of ethanol and the frequency of the four formants of the sensor was analyzed and applied to the determination of the mole fraction of ethanol solution. Compared with the commonly used chemical methods, this method has the advantages of rapidness and non-destruction of samples. Because the sensor measures the mole fraction according to the change of the absorption coefficient of the liquid to be measured, the conclusion of this work can be extended to the mole fraction detection of other mixed solutions. These conclusions are of certain significance to promote the application of terahertz spectral detection technology in the fields of trace substance detection, biosensor, drug reaction and in vivo monitoring.

Acknowledgments

This work is supported by Natural Science Foundation of Guangdong Province(No. 2022A1515011409); supported by Support for scientific research projects (scientific research projects in colleges and universities) (No. 2019KTSCX165); supported by Foundation Funded Project of doctoral(No.99000617); supported in part by research grants from the Science and Technology Program of Shaoguan (No. 2019sn056; 2019sn066); supported in part by the Key platforms and major scientific research projects of Universities in Guangdong (No.2017KQNCX183); supported in part by the Key Project of Shaoguan University (No. SZ2017KJ08; SZ2020KJ02); supported in part by Youth Project of National Natural Science Foundation of China (No.62001200), supported in part by the Natural Science Foundation of Fujian Province (No.2020J01817); supported in part by Science and Technology Program of Shaoguan (No.200811094530423,200811094530805,210726214533586 and 200811094530811).

References

[1] J. B. Pendry, Contemporary Physics **45**(3), 191 (2004).
[2] W. Withayachumnkul, D. Abbott, IEEE Photonics Journal **1**(2), 99 (2009).

[3] Yaru Wang, Lanju Liang,Maosheng Yang,Xujuan Wang,Yan Wang, Laser& Optoelectronics Progress **56**(4), 041603 (2019).
[4] Xiaojun Wu ,Baogang Quan ,Xuecong Pan , Xinlong Xu, Xinchao Lu, Changzhi Gu , Li Wang, Biosensors and Bioelectronics **42**, 626 (2013).
[5] Lijuan Xie, Weilu Gao, Jie Shu, Yibin Ying, Junichiro Kono, Scientific Reports **5**, 8671 (2015).
[6] A. Yang, Z. Li, M. P. Knudson, A. J. Hryn, W. Wang, K. Aydin, T. W. Odom, Nano **9**(12), 11582 (2015).
[7] Fangrong Hu, Enze Guo, Xin Xu, Peng Li, Xinlong Xu, Shan Yin, Yuee Wang, Tao Chen, Xianhua Yin, Wentao Zhang, Optics Communications **388**, 62 (2017).
[8] M. Chen, L. Singh, N. Xu, R. Singh, W. Zhang, L. Xie, Optics Express **25**(13), 14089 (2017).
[9] Jikai Xu, Zhihao Ren, Bowei Dong, Xinmiao Liu, Chenxi Wang, Yanhong Tian, Chengkuo Lee, ACS Nano **14**(9), 12159 (2020).
[10] Zhihao Ren, Yuhua Chang, Yiming Ma, Kailing Shih, Bowei Dong, Chengkuo Lee, Adv. Optical Mater. **8**(3), 1 900653 (2020).
[11] Jingxuan Wei, Zhihao Ren, Chengkuo Lee, J. Appl. Phys. **128**, 240901 (2020).
[12] Yuhua Chang, Jingxuan Wei, Chengkuo Lee, Nanophotonics **9**(10), 0045 (2020)
[13] Yiming Ma, Bowei Dong, Chengkuo Lee, Nano Convergence **7**, 12 (2020).
[14] Yu-Sheng Lin, Zefeng Xu, International Journal of Optomechatronics **14**(1), 78 (2020).
[15] Jikai Xu, Yunchen Du, Chenxi Wang, International Journal of Optomechatronics **14**(1), 94 (2020).
[16] Lei Liu, Zhenguo Jiang, Syed Rahman, Md. Itrat Bin Shams, Benxin Jing, Akash Kannegulla, Li-Jing Cheng, Micromachines **7**(5), 75 (2016).
[17] Qi Tang, Min Liang, Yi Lu, Pak Kin Wong, Gerald J. Wilmink, Donna D. Zhang, Hao Xin, Sensors **16**(4), 476 (2016).
[18] S. J. Park, S. A. N. Yoon, Y. H. Ahn, RSC Advances **6**(73), 69381 (2016).
[19] Xin Hu, Gaiqi Xu, Long Wen, Huacun Wang, Yuncheng Zhao, Yaxin Zhang, David R. S. Cumming, Qin Chen, Laser & Photonics Reviews **10**(6), 962 (2016).
[20] Li Liang, Xin Hu, Long Wen, Yuhuan Zhu, Xianguang Yang, Jun Zhou, Yaxin Zhang, Ivonne Escorcia Carranza, James Grant, Chunping Jiang, David R. S. Cumming, Baojun Li, Qin Chen, Laser & Photonics Reviews **12**(11), 1800078 (2018).
[21] Zhaoxin Geng, Xiong Zhang, Zhiyuan Fan, Xiao Qing Lv, Hongda Chen, Scientific Reports **7**, 16378 (2017).
[22] Kailing Shih, Prakash Pitchappa, Lin Jin, Chia-Hung Chen, Ranjan Singh, Chengkuo Lee, Applied Physics Letters **113**(7), 071105 (2018).
[23] CST microwave studio. HTTPs://www.cst.com/products/cstmws.
[24] Yogesh Kumar Srivastava, Apoorva Chaturvedi, Manukumara Manjappa, Abhishek Kumar, Govind Dayal, Christian Kloc, Ranjan Singh, Advanced Optical Materials **4**(3), 457 (2016).
[25] X. C. Lu, J. G. Han, W. L. Zhang, IEEE Journal of Selected Topics in Quantum Electronics **17**(1), 119 (2011).
[26] J. T. Kindt, C. A. Schmuttenmaer, Journal of Physical Chemistry **100**(24), 10373 (1996).
[27] M. Swithenbank, A. Burnett, C. Russell, Lianhe Li, A. Davies, E. Linfield, J. Cunningham, C. Wood, Analytical Chemistry **89**(15), 7981 (2017).
[28] Peter Uhd Jepsen, Uffe Møller, Hannes Merbold, Optics Express **15**(22), 14717 (2007).
[29] R. C. Fang, Solid spectroscopy, Hefei University of Science and Technology of China Press, 1 (2001).

*Corresponding author: liujianjun@swu.edu.cn